TRAIL Coated Genetically Engineered Immunotherapeutic Nano-Ghosts (iNGs) Vesicles Target Human Melanoma and Avoiding the Need for High Effective Therapeutic Concentration of TRAIL.

Lior Levy,* Tzila Davidov, Krishna K. Kolluri, Avraham Fridman, Stasia Krishtul, Sam M. Janes, Marcelle Machluf *

Affiliations:

Dr. L. Levy, T. Davidov, A. Fridman, Dr. S. Krishtul, Prof. M. Machluf

Faculty of Biotechnology and Food Engineering, Technion – Israel Institute of Technology, Haifa 32000, Israel

Dr. K.K. Kolluri, Prof. S.M. Janes

Lungs for Living Research Centre, UCL Respiratory, Division of Medicine, University College London, London, UK

Keywords: Mesenchymal stem cells, Melanoma, TRAIL, Nano-Ghosts, Nanovesicles.

Cancer cell therapy using cytotoxic T lymphocytes (CTL) or mesenchymal stem cells (MSC) possesses hurdles due to the cells susceptibility to host induced changes. Here, a versatile inanimate broadly applicable nanovesicles, termed Immunotherapeutic-Nano-Ghosts (iNGs), armed with inherent surface-associated targeting and therapeutic capabilities in which the promise and benefits of MSC therapy and T cell immunotherapy are combined into one powerful off-the-shelf approach for treating malignant diseases. To mimic the cytotoxic or immunosuppressive functions of T cells, iNG are produced from MSC that were genetically engineered (G.E) or metabolically manipulated to express additional membrane-bound proteins, endowing the NGs derived therefrom with additional surface-associated functions such as

tumor necrosis factor (TNF)-related apoptosis-inducing ligand (TRAIL). iNGs from G.E-MSCs (G.E-iNGs) show superior TRAIL retention and induce apoptosis in different cancer cell lines *in vitro*. *In vivo* studies on a human melanoma model demonstrate that a systemic, three-day frequency, administration of G.E-iNGs result in tumor inhibition comparable to six orders-of-magnitude higher concentration of soluble TRAIL. The iNGs are therefore a promising nanovesicle platform that can affect tumors in a non-immunogenic manner while avoiding the need for high effective therapeutic concentration.

1. Introduction

Current cancer immunotherapies are focused on activating and enhancing cytotoxic T lymphocytes (CTLs) response specifically towards the patients' tumor.[1,2] CTLs use two main pathways to induce apoptosis in their target cells; by the secretion of serine proteases termed granzymes (e.g. granzyme B), and via the death ligand/ death receptor pathway using Fas-ligand (FasL) or tumor necrosis factor (TNF)-related apoptosis-inducing ligand (TRAIL) by recruiting the death-inducing signaling complex (DISC).[3] Unfortunately, in the face of widely variable and adaptive tumors, often presenting a highly immunosuppressive environment and major histocompatibility complex (MHC)-restriction, the possible use of CTLs is largely limited to a small number of patients and very few types of cancers.[4]

In recent years, much effort has been devoted to the use of TRAIL as a therapeutic agent to treat cancer.[5–8] TRAIL is a type II transmembrane protein able to selectively trigger apoptosis in cancer cells, while not affecting normal cells due to multiple redundant pathways in the non-malignant cells.[9] The soluble form of TRAIL (sTRAIL) has been studied extensively and tested in clinical trials,[10,11] however, low bioavailability, poor pharmacokinetics, short half-life, and resistance to TRAIL resulted in unsatisfactory clinical performance. [10,11] For these reasons, attempts to increase sTRAIL bioavailability were made by using targeted delivery approaches. sTRAIL has been delivered to the tumor site by various vectors such as

cells,[5,7,12,13] liposomes[13–16] and membrane-derived nanoparticles[17,18] and showed remarkable results. In several studies, membrane-bound TRAIL was considered even more effective than its soluble counterpart, as ligand oligomerization was found to be a key element in efficient induction of apoptosis.[19,20] Therefore, it came as no surprise that TRAIL-coated vectors proven highly efficient in inducing apoptosis, even in TRAIL resistant tumors.[7,21] However, most of these approaches rely on passive targeting[21] while the majority of those who use active targeting, require the incorporation of an additional targeting moieties (e.g. scFv) which may create challenges when moving to clinical settings.[22]

One of the highly adopted cellular vectors used today for cancer treatment are mesenchymal stem cells (MSCs).[23,24] This is due to their ability to traverse physiological barriers, and target different sites of inflammation, including primary and metastatic tumors, while exhibiting relative allogeneic safety.[25] Building on these capabilities, MSCs manipulated *ex vivo* to secrete anti-neoplastic factors have been tested as cell carriers for treating cancer.[26,27] However, once in the patient's body, MSCs may undergo changes that reshape their targeting capabilities or increase their immunogenicity, minimizing their overall effect.[28] Moreover, as MSCs are able to protect the tumor from the immune system and promote the metastatic process, they may, unfavorably, expedite tumorigenesis.[29]

We have previously developed a novel class of targeted nanoparticles termed Nano-Ghosts (NGs), which are reconstructed from the cytoplasmic membranes of MSCs.[18,30,31] NGs present a more scalable and robust approach and have better loading abilities, compared to biologically derived extracellular vesicles (EVs).[32] For example, EVs and NGs different manufacturing process, EVs being shed or bud from cells while NGs are manufactured through mechanical and physical disruption of cell membranes, controls the characteristics of each vesicle type. More specifically, while the NGs are lacking any cytoplasmic content of their source cells, EVs still contain their origin cell RNA.[33] In addition, EVs membranes do not represent the full composition of their source cell membrane, and are often enriched with proteins from sources

related to their biogenesis.[34] on the other hand, the composition, orientation, and functions associated with MSC membranes, which largely govern their therapeutic potential, are retained by the NGs and in particular, the ability to actively home in on and infiltrate malignant tissues, while rapidly clearing from other organs with no apparent off-target effects.[18,30,35] This may give a significant advantages to the NG system over other biological and synthetic particulates. In this study we have advanced the NG technology by genetically manipulating the NG membrane surface to express additional and or desired therapeutic protein which can mimic the activity of different cells than MSCs. Such modifications, we hypothesize, can be implemented to create a new class of immunotherapeutic NGs (iNG) with capabilities inspired by CTLs, in particular, with an expressed coating of membrane proteins, such as the death ligand TRAIL. This will enable the iNGs to target cancer cells, as well as eradicate them without the need to use the patient own cells. In this work, we demonstrate the targeting and therapeutic efficacy of such unique iNGs on a melanoma tumor model.

2. Results and discussion

iNGs were produced from MSCs which were manipulated to express membrane-bound full-length TRAIL. Manipulation of MSCs to express TRAIL was performed either via activation of the cells by TNFα or through genetic engineering of MSC (G.E; **Figure 1**). First, we observed that TRAIL expression was upregulated after activation of MSCs by 10 ng/ml of TNFα for 24 hours (TNFα-activated MSCs) as was previously published by Lee *et al*., 2012,[12] detecting 20% higher levels of TRAIL in TNFα-activated MSCs compared to control (**Figure 2**A). To study whether the TNFα-activated MSCs can induce cell death in cancer cells, Jurkat cells were co-cultured with activated and inactivated MSCs in a direct and indirect co-culture. As expected, Jurkat cell death was significantly higher (35% ± 1.5) in a direct co-culture with TNFα-activated MSCs compared to a direct co-culture with inactivated MSCs (13.8% ± 0.2; $P< 0.005$) and compared to an indirect co-culture with TNFα-activated MSCs (20.0% ± 0.6; $P< 0.01$;

Figure 2B), indicating that the effect on viability is caused by a contact-based mechanism. Interestingly, light microscopy images revealed that Jurkat cells bind to TNFα-activated MSCs membrane, as opposed to inactivated MSCs (Figure 2C), this may be due to interactions between TRAIL and TRAIL receptor and should be further studied. Next, we studied murine and human cancer cell lines sensitivity to human recombinant soluble TRAIL (sTRAIL), with the aim to choose the best solid tumor cancer model for the iNGs studies. Murine and human cancer cell lines were incubated with two concentrations of human sTRAIL (100 and 1000 ng/ml) and tested for their viability after 24 hours.[36] For these studies, human and murine lung carcinoma (A549 and LLC), breast adenocarcinoma (MDA-231 and 4T1), glioma cells (U87 and GL-261), and human melanoma (113/6-4L) were used. Human smooth muscle cells (SMC) were used as a non-cancerous control. Our data confirmed that human sTRAIL is significantly more effective against human cell lines than murine cell lines, which were not affected by the human sTRAIL (Figure 2D). This correlates with the fact that the human TRAIL protein has only 65% homology to murine TRAIL, and murine cell lines have only one TRAIL receptor compared to two in human cells and therefore are less sensitive.[37] Amongst the human cell lines, melanoma 113/6-4L, breast adenocarcinoma MDA-MB-231 (MDA-231) and U87 glioma cells were found to be highly sensitive to sTRAIL compared to A549 lung cancer cells (Figure 2D), which is known to be TRAIL-resistant.[7,38] To study the effect of iNGs produced from TNFα-activated MSCs (TNFα-iNGs) on cancer cell death, the TRAIL-sensitive MDA-231 cells were incubated with NGs produced from unmodified MSCs (MSC-NGs) or NGs produced from TNFα-activated MSCs (TNFα-iNGs) for 24 hours in two concentrations (10 or 20 μg lipids/ml; Figure 2E). MDA-231 cells viability was significantly reduced in a dose-dependent manner after treatment with TNFα-iNGs compared to MSC-NGs (0.88 ± 0.04 fold, $P<0.01$ and 0.74 ± 0.06 fold, $P<0.005$, respectively), with 20 μg lipids/ml being significantly more effective than the lower concentration ($P<0.005$), proving that TNFα-iNGs are able to affect cancer cells viability. However, expression of TRAIL after activation of MSCs using TNFα is considered

weak, inconsistent and could change drastically from donor to donor.[12] Therefore, we also used a second approach to manipulate MSCs to express full length membrane TRAIL using genetic engineering.[7,39] We used genetically engineered MSCs expressing full-length TRAIL (G.E MSCs-TRAIL), previously shown to express intracellular and membrane bound TRAIL and to induce apoptosis in TRAIL-sensitive and TRAIL-resistant cancer cell-lines.[7] Indeed, G.E MSCs-TRAIL expressed typical MSC markers as their unmodified variants and very high levels of membrane bound TRAIL (65%; **Figure 3**A), significantly higher than the expression that was achieved using the TNFα method (Figure 2A). Next, the effect of G.E MSC-TRAIL on human cancer cell-lines was assessed using flow cytometry. MSCs and G.E MSC-TRAIL were co-cultured for 24 hours with different human cancer cell lines and tested for apoptosis. As seen, co-culture with G.E MSC-TRAIL resulted in a significant induction of apoptosis ($Annexin^+/PI^+$) in all cancer cells tested compared to co-culture with unmodified MSCs (A549 31%; 113/6-4L 51%; MDA-231 32%; U87 45%; $P<0.001$, Figure 3B), confirming the lethal effect of the G.E cells on those cancer cells which originated from both soluble and contact dependent mechanisms (Figure 2D). [7]

Characterization of the physical properties of the NGs provided evidence to their stability and membrane composition. The iNGs produced from G.E MSCs-TRAIL (G.E-iNGs) exhibited size distribution of 191.3±3.0 nm (**Figure 4**A), similar to the size distribution of MSC-NGs which is ~180nm (not shown).[18] NG-morphology was evaluated using cryo-TEM and depicting a unilamilar and spherical shape, decorated with proteins (Figure 4B). MSC markers (CD90, CD29, CD44 and CD105) were retained on the iNGs (35, 61, 68 and 10%, respectively), and TRAIL was detected on their surface (24%), as shown by flow cytometry analysis using Dynabeads conjugated to the iNGs and immunostained (Figure 4C). G.E-iNGs zeta potential was found to be -23±1.6 mV (not shown) compared to MSC-NGs zeta potential which was shown to be -20 mV.[40] These results indicate that the genetic engineering process of the MSCs

did not alter the MSC-NGs properties, and the newly formed G.E-iNGs is coated by TRAIL and can potentially exert apoptosis to cancer cells.

Next, we have studied the G.E-iNGs effect on various human cancer cell lines. MSC-NGs and G.E-iNGs (10 μg lipids/ml) were incubated separately with human cancer cell lines and viability was assessed after 48 hours. 113/6-4L and MDA-231 viability was significantly reduced by the G.E-iNGs treatment compared to treatment with MSC-NGs (68% and 30%, respectively, $P<0.05$) while A549 and U87 cells did not respond to the treatment (**Figure 5**A). Examination of the expression of TRAIL receptors on the surface of the different cancer cells using flow cytometry may explain this result. While TRAIL has five receptors to which it can bind, only two of them are functional and can induce apoptosis (TRAIL-R1 and TRAIL-R2), while three act as decoys (TRAIL-R3, TRAIL-R4 and OPG). The decoy receptors lack the cytoplasmic functional death domain that TRAIL-R1 and TRAIL-R2 possess, which is essential for the induction of apoptosis. TRAIL-R3 and TRAIL-R4 have been suggested to inhibit induced apoptosis by a process called ligand-scavenging or by cooperating with the anti-apoptotic regulator cellular-FLICE inhibitory protein (c-FLIP). [21,41,42] Unsurprisingly, the cells that were found to be most sensitive to G.E-iNGs, MDA-231 and 113/6-4L, also expressed low levels of TRAIL-R4 decoy receptor (0 and 25%, respectively; Figure 5B), and did not express TRAIL-R3 decoy receptor. In addition, MDA-231 and 113/6-4L cells were found to express the functional TRAIL receptors TRAIL-R1 (17 and 55%, respectively) and TRAIL-R2 (85 and 99%, respectively), as previously shown.[43] The higher level of TRAIL-R4 and lower level of TRAIL-R1 in 113/6-4L cells compared to MDA-231 cells may explain the higher effect on MDA-231 viability by the G.E-iNGs. Furthermore, U87 cells, which highly express TRAIL-R2 (99%), were also found to highly express the decoy receptor R4 (61%), consistent with previous work by Menon et al and thereby explaining their lack of effect by the G.E-iNGs.[44] Interestingly, A549 cells were found to express high levels of TRAIL-R1 and TRAIL-R2 (80 and 98%, respectively), low levels of the decoy receptors TRAIL-R3 (5%) and medium level

of the decoy receptors TRAIL-R4 (36%). Although A549 cells highly express the functional TRAIL receptors, they are still considered TRAIL-resistant and did not respond to the G.E-iNGs (Figure 5A). [45,46] The main reason for A549 resistance is attributed to the expression of anti-apoptotic proteins such as mcl and c-FLIP, as it was found that inhibiting these two proteins in the cells would result in TRAIL-dependant apoptosis.[47,48]

To compare the effect of both TNFα-iNGs and G.E-iNGs on cancer cells, we incubated the TRAIL-sensitive cell-lines 113/6-4L and MDA-231 with the two types of iNGs (TNFα and G.E; 10 μg lipids/ml) for 24 hours and analyzed the tumor cells' apoptosis levels compared to untreated control. G.E-iNGs treatment of both cancer cell types showed high apoptosis fold change while not affecting the non-cancerous SMC (Figure 5C). However, treatment with TNFα-iNGs did not show any significant effect on apoptosis in comparison to treatment with MSC-NGs (Figure 5C). This can be explained by the higher expression of TRAIL on the G.E-MSCs surface compared to TNFα-activated MSCs and thereby its higher retention on the iNGs membranes. This emphasizes the benefits of using the genetic engineering approach in comparison to activation by TNFα, the latter shows less consistent results and thereby less suitable for *in vivo* studies.

Among the two TRAIL-sensitive cell lines we have tested in this work, 113/6-4L cells were selected as our *in vivo* model as they express the TRAIL-R4 decoy receptor (Figure 5B); the rational is that they present a bigger challenge than MDA-231 cells that do not express any decoy TRAIL receptors. G.E-iNGs and free human sTRAIL (300 μg sTRAIL/mouse) were injected into tumor-bearing severe combined immuno-deficient (SCID) mice in a three-day injection regiment (**Figure 6**A). Three intravenous (*i.v*) injections of G.E-iNGs resulted in a significant inhibition of tumor growth compared to untreated mice ($P<0.001$; Figure 6B). Remarkably, the tumor inhibition achieved by the G.E-iNGs was similar to the one achieved by a systemic administration of sTRAIL (300 μg/mouse), however, TRAIL administered to the

mice via the G.E-iNGs treatment only ranged between 270-740 pg/mouse as verified by ELISA (Figure 6C). This 6-orders of magnitude difference in TRAIL concentration can be associated with the iNGs targeting ability; While sTRAIL's poor pharmacokinetics allows it to inflict a short and untargeted response, [17,49,50] the iNGs targeting properties allows it to accumulate in the tumor bulk[30] and lower the effective concentration of TRAIL.

Tumors from animals treated with G.E-iNGs were found to express less Ki-67 and CD31, and higher levels of caspase 3 than the controls, indicating less proliferation and vascularization, and more induced apoptosis compared to untreated mice and to mice treated with sTRAIL (Figure 6C). Quantitative analysis of the immunohistochemistry (IHC) micrographs using the Andy's algorithm[51] validated these results (Figure 6E-G). Interestingly, mice bearing tumors and treated with sTRAIL did not show an increase in caspase 3 levels nor a decrease in Ki-67 and CD31. This can be explained by the H&E results that shows an intact tissue, without visible necrosis which indicate that although the sTRAIL treatment inhibited tumor growth progression it did not kill the cells.

In the immunogenicity studies, alanine transaminase (ALT) measurement of serum samples taken from tumor-bearing SCID mice treated with G.E-iNGs and free sTRAIL showed ALT levels that are normally obtained for a non-toxic drug (<40 U/ml; **Figure 7**A).[52,53] H&E staining from liver samples taken from mice treated with G.E-iNGs or sTRAIL showed no apparent toxicity compared to untreated SCID mice (Figure 7B). In addition, the inflammatory cytokines TNF-α, INF-γ, IL1-β and IL-6 levels did not rise in C57/BL mice treated with G.E-iNGs up to three weeks post injection compared to untreated mice (Figure 7C). As their unmodified variants, [30] the G.E-iNGs retains the stealth properties of the MSCs and do not induce liver cytotoxicity in treated mice, bringing them closer to becoming an off-the-shelf treatment.

3. Conclusions

In conclusion, the iNGs can mimic membrane-bound lethal effect of CTLs while featuring the active targeting properties of MSCs, all in a non-immunogenic platform that does not require autologous cells. The G.E-iNGs, which were produced from MSCs that were genetically engineered to express TRAIL on their surface, could induce apoptosis in cancer cells and significantly inhibit tumor growth in a melanoma model without detectable toxicity. G.E-iNGs showed better *in vitro* results than their TNFα-iNGs counterparts and their *in vivo* effect was comparable to the one obtained from 6 order of magnitudes higher concentration of sTRAIL. The iNGs ability to affect cancer cells *in vitro* and *in vivo*, while sparing non-cancerous cells and maintaining the safety and tumor targeting of the MSCs, can undoubtedly make them the new standard for NGs cancer treatment that would be further combined with anti-cancerous loaded drugs.

4. Experimental Section

Cell Cultures:

Unmodified human bone marrow mesenchymal stem cells (MSCs) were purchased from Lonza™ (Basel, Switzerland). MSCs and human smooth muscle cells (SMC; Isolated from human bladder) were cultured in alpha-mem (α-mem) and high-glucose DMEM, respectively (Biological Industries, Beit Ha'Emek, Israel), and supplemented with 5 ng/ml basic fibroblast growth factor (bFGF, Peprotech, Rehovot, Israel). Non-small cell lung cancer cells (A549, ATCC #CCL- 185™) and Jurkat cells (kindly donated by Professor Ben-Zion Levi from the Faculty of Biotechnology and Food Engineering, IIT, Israel) were grown in RPMI-1640 (Sigma-Aldrich™). Lewis lung carcinoma cells (LLC, ATCC CRL-1642™), metastatic human melanoma cell line 113/6-4L (kindly donated by Professor Eva Hernando, Department of Pathology, NYU Langone Medical Center, NY, USA.), human breast adenocarcinoma epithelial cells MDA-MB-231 (MDA-231, kindly donated by Professor Gera Neufeld, Department of Anatomy and Cell Biology, Faculty of Medicine, IIT, Israel), murine

glioblastoma cells GL261 (obtained from the NCI-Frederick Cancer Research, NIH, Maryland, USA) and 4T1 mouse mammary tumor cell line (ATCC CRL-2539™) were cultured with high-glucose DMEM (Biological Industries). Human glioblastoma epithelial cells (U87 MG, ATCC® #HTB14) were cultured with Mem-Eagle medium (Biological Industries). All culture media were also supplemented with 10% fetal bovine serum (FBS), 1% Pen-Strep solution and 0.8% Amphotericin B, all purchased from Biological Industries.

Transduction of MSCs:

Transduction of MSCs with lentiviral particles containing TRAIL plasmid was performed as previously published.[7]

Preparation of NGs and iNGs:

NGs and iNGs were produced, as we have previously published with minor changes,[30] from three different source cells: unmodified human bone marrow MSCs, MSCs pre-activated by TNFα and genetically engineered MSCs that expresses full length TRAIL. Briefly, MSCs were harvested, washed with PBS, and re-suspended in a hypotonic Tris- Magnesium buffer (TM-buffer, pH 7.4, 4ºC) containing 10 mM Tris and 1 mM MgCl2 (Sigma-Aldrich™). Cells were homogenized at 8,800 rpm for 60 sec (DIAX100 homogenizer, Heidolph Instruments) and immediately after the homogenization, a sucrose (Sigma-Aldrich™) solution in TM-buffer (60% w/v) was added, to a final concentration of 0.25M. The homogenized cells were then centrifuged at 2400g for 40 min at 4°C. The supernatant was discarded and the resulting pellet, containing the cell ghosts, was centrifuged and washed twice more with 0.25M sucrose in TM-buffer (pH 7.4). The re-suspended pellet was than sonicated for 5 sec at 27% amplitude using a VibraCell VCX750 (Sonics & Materials Inc., Newtown, CT) and centrifuged at 2400g for 40 min at 4°C. The pellet was washed twice more with 0.25M sucrose in TM-buffer pH 8.6 as before. To downsize the ghosts into NGs or iNGs, the re-suspended pellet, containing the ghost

vesicles, was sonicated for 2 min at 27% amplitude and centrifuged at 800g for 10 min at 4°C. The pellet was discarded and the supernatant containing the NGs was filtered through 0.45 μm syringe filters and ultra-centrifuged at 150,000g for 45 min at 4°C. The resulting NG pellet was re-suspended in PBS. The NGs were then PEGylated, as we published before,[18] and the final NGs product was resuspended in PBS. The amount of phospholipids in the NG samples was determined using a LabAssay™ phospholipid kit (Wako, Osaka, Japan).

iNGs Characterization:

The size, size distribution and NGs concentration were determined using NanoSight NS300 (Malvern, Malvern Instruments, Malvern-Worcestershire, United Kingdom). The Zeta-potential of NGs was analyzed using Zetasizer® Nano-Series® (Malvern Instruments). iNGs Samples were imaged by Cryo-TEM (Philips CM120, 120 kV) using an Oxford CT-3500 Cryo-holder and digitally recorded, as we previously published.[18] To validate the retention of membrane markers on the iNGs surface, NGs were covalently adsorbed to the surface of Tosyl-activated M-280 Dynabeads™ (Invitrogen™) according to the manufacturer's protocol with adjustments, as previously published by Bronshtein et al.[54] iNG-conjugated beads were analyzed by flow cytometry for typical MSC markers (Biolegend) and TRAIL (BD) against isotype controls.

Co-culture of modified MSCs and cancer cell lines:

MSCs were seeded (10^4 cells/cm^2) in 6 well plate and allowed to grow overnight in complete culture media (CCM; α-MEM supplemented with 17% FBS, 2mM L-Glutamine, 1% P/S and 0.8% Amphotericin B). The next day, Jurkat cells were cultured with or without the MSCs (ratio 4:10 MSC: Jurkat) in a direct or indirect manner (Transwell, 0.4 mm pore size; Merck, Germany) in culture media (CM; α-MEM supplemented with 2% FBS, 2mM L-Glutamine, 1% P/S and 0.8% Amphotericin B) with or without TNFα (10 ng/ml, Peprotech) as was described

by Hwa Lee *et al*.[12] After 24 hours, supernatants were collected, and Jurkat cells were incubated with 1 µg/ml propidium iodide (PI.; Sigma Aldrich) prior to flow cytometry. In another experiment, unmodified MSCs and genetically engineered (G.E) MSCs expressing TRAIL were mixed with DiD lipophilic fluorescent dye (ThermoFisher), to a final concentration of 1.25µg/ml, for 2 hours prior to seeding. Then, cells were seeded ($2.5 \cdot 10^4$ cells/cm^2) in 96 well plate and allowed to grow overnight. The next day, cancer cells (A549, MDA-231, 113/6-4L and U87) were cultured with or without the MSCs (ratio 4:10 MSC: cancer). After 24 hours, supernatants were collected, and cancer cells (DiD negative) were analyzed for apoptosis using flow cytometry (FACS Calibur, BD) using Annexin V-fluorescein isothiocyanate (FITC) Apoptosis Detection Kit (MBL International Corp., Woburn, MA) according to the manufacturer's instructions.

Cancer cells sensitivity to sTRAIL:

A549, LLC, MDA-231, 4T1, U87, GL261, 113/6-4L and SMC were seeded ($2.5 \cdot 10^4$ cells/cm^2) in 96 well plate and allowed to grow overnight. The next day, cells were incubated with recombinant human sTRAIL (100 and 1000 ng/ml, Peprotech) for 24 hours. Cell viability was followed up using the AlamarBlue™ assay (Invitrogen™); Cell growth media supplemented with AlamarBlue™ reagent (1:10) for 2 hours. Fluorescence (excitation: 530/30 nm emission: 590 nm) was measured on a microplate reader. The relative cell viabilities were then calculated in respect to the untreated control, set as 100%.

iNGs targeting studies:

Target cells were seeded ($2.5 \cdot 10^4$ cells/cm^2) in 96 well plate and allowed to grow overnight. MSC-NGs and iNGs (10 or 20 µg lipids/ml) were incubated with the target cells for 24 or 48 hours. Cell viability was followed up using the AlamarBlue™ assay (Invitrogen™); Cell

growth media supplemented with AlamarBlue™ reagent (1:10) for 2 hours. Fluorescence (excitation: 530/30 nm emission: 590 nm) was measured on a microplate reader. The relative cell viabilities were then calculated in respect to MSC-NGs. Alternatively, detection and apoptosis levels of cells was performed using the ApoTox-Glo™ assay according to manufacturer's recommended protocol (Promega) using a plate reader. The relative cell apoptosis levels were then calculated as the log fold change in respect to untreated control.

Flow cytometry analyses:

Cells were thoroughly washed with PBS and then incubated with Trypsin-EDTA for 5 minutes at 37 °C to detach them from plate surface. An equal volume of culture media was used to neutralize the protease at the end of the trypsin treatment. Cells ($2 \cdot 10^5$) were then washed twice with PBS supplemented with 0.5% bovine serum albumin (BSA, MP Biomedicals, USA) and cells were incubated with appropriate antibodies (Biolegend, BD bioscience or R&D Systems) for 30 minutes on ice. Cells were washed twice again with PBS-BSA and a total of $1 \cdot 10^5$ events were recorded using FACS Calibur (BD) and analyzed by FCS Express (De Novo Software, Los Angeles, CA).

In vivo efficacy and immunogenicity studies:

All animal experiments were carried out in compliance with the Council of Animal Experiments, and the Israel Ministry of Health guidelines for the care and use of laboratory animals, and under animal ethics committee approval No. IL-062-05-2019.

Seven-week-old male severe combined immuno-deficient (SCID) mice were inoculated subcutaneously in the flank with $1 \cdot 10^6$ 113/6-4L cells. Tumors volumes were measured using a caliper during the experiment and calculated according to the following correlation: $Volume = Lenght \cdot Width^2 \cdot 0.5$, as previously published.[55] When tumors reached an average volume of 150 mm^3, animals were randomly divided into three groups: Untreated control, mice

injected (*i.v.*) with recombinant soluble TRAIL (300 µg/mouse) and G.E-iNGs (0.5 mg/kg). injection of treatment and controls were performed every three days (days 0, 3, 6). Tumor sizes were followed until 3 days post last treatment administration (day 9), after which mice were sacrificed, the percentage of change in tumor size from the day of the first injection was calculated and tumors were extracted. Tumors and livers were directly embedded in formalin solution (#HT-501128, Sigma), and were sliced into 10-µm-thick sections using a cryostat for further analyses. To determine G.E-iNG effect on tumor pathology, tumor and liver slices were subjected to pathological (H&E) and tumors were also subjected to immunohistochemical (IHC) analysis for apoptosis (caspase-3, Abcam) proliferation (KI-67, Abcam) and vascularization (CD31, Abcam). IHC indices were calculated from the micrographs (n=30 samples/group) using the "Andy's Algorithm"[51] on ImageJ based Fiji software. Sectioning of the tumors and H&E staining were performed by the Biomedical Core Facility at the Rappaport Faculty of Medicine, IIT.

For the immunogenicity studies, the blood serum from mice treated as described above was separated and analyzed for alanine transaminase (ALT) levels using Alanine Transaminase Colorimetric Activity Assay Kit (Cayman Chemicals) according to the manufacturer's protocol. To assess immune response, seven-week-old male C57BL mice were divided into two groups: a control group, administered with 100 µl PBS on day 0; and a group administered once with G.E-iNGs (0.5 mg/kg) at day 0. Mice from the control and treatment groups were sacrificed at day 7 and 21 (3 and 5 mice, respectively) and their blood was collected. Blood levels of IL-1β, IL-6, INF-γ and TNF-α were assessed using Milliplex Mouse Cytokine/Chemokine Magnetic Bead Panel (MCYTOMAG-70K-03, Millipore) according to the manufacturer's protocol.

Statistical analysis

Results are presented as the mean ± SD (standard deviation) of at least triplicates. Statistical significance in the differences of the means was evaluated by a two-tailed t-test.

Acknowledgements

This work was supported by the Israel Science Foundation (ISF) [grant number 1673/17]. L.L was supported by the Israeli Scholarship Education Foundation (ISEF) and the Planning and Budgeting committee in Israel. L.L. and M.M designed the experiments, L.L carried out the experiments and analyzed the data. T.D. carried out the CD31 IHC staining. K.K. transduced and provided the genetically engineered MSCs expressing full length TRAIL. A.F and S.K assisted with the *in vivo* experiments. L.L. and M.M. wrote the manuscript. M.M. supervised the study.

Received: ((will be filled in by the editorial staff))
Revised: ((will be filled in by the editorial staff))
Published online: ((will be filled in by the editorial staff))

References

[1] C. G. Drake, E. J. Lipson, J. R. Brahmer, *Nat. Rev. Clin. Oncol.* **2014**, *11*, 24.

[2] M. E. Dudley, S. A. Rosenberg, *Nat. Rev. Cancer* **2003**, *3*, 666.

[3] L. Martinez-Lostao, A. Anel, J. Pardo, *Clin. Cancer Res.* **2015**, *21*, 5047.

[4] K. Fousek, N. Ahmed, *Clin. Cancer Res.* **2015**, *21*, 3384.

[5] K. K. Kolluri, G. J. Laurent, S. M. Janes, *Respiration* **2013**, *85*.

[6] R. M. Thakrar, E. K. Sage, S. M. Janes, *Expert Opin. Biol. Ther.* **2016**, *16*, 853.

[7] Z. Yuan, K. K. Kolluri, E. K. Sage, K. H. C. Gowers, S. M. Janes, *Cytotherapy* **2015**, *17*, 885.

[8] O. Micheau, S. Shirley, F. Dufour, *Br. J. Pharmacol.* **2013**, *169*, 1723.

[9] M. van Dijk, A. Halpin-McCormick, T. Sessler, A. Samali, E. Szegezdi, *Cell Death Dis.* **2013**, *4*, e702.

[10] S. von Karstedt, A. Montinaro, H. Walczak, *Nat. Rev. Cancer* **2017**, *17*, 352.

[11] J. Lemke, S. von Karstedt, J. Zinngrebe, H. Walczak, *Cell Death Differ.* **2014**, *21*, 1350.

[12] R. H. Lee, N. Yoon, J. C. Reneau, D. J. Prockop, *Cell Stem Cell* **2012**, *11*, 825.

[13] P. M. Nair, H. Flores, A. Gogineni, S. Marsters, D. A. Lawrence, R. F. Kelley, H. Ngu, M. Sagolla, L. Komuves, R. Bourgon, J. Settleman, A. Ashkenazi, *Proc Natl Acad Sci U S A* **2015**, *112*, 5679.

[14] D. De Miguel, A. Gallego-Lleyda, J. M. Ayuso, S. Erviti-Ardanaz, R. Pazo-Cid, C. del Agua, L. J. Fernández, I. Ochoa, A. Anel, L. Martinez-Lostao, *Nanotechnology* **2016**, *27*, 185101.

[15] D. De Miguel, A. Gallego-Lleyda, M. Martinez-Ara, J. Plou, A. Anel, L. Martinez-Lostao, *Cancers (Basel).* **2019**, *11*, 1948.

[16] L. Martinez-Lostao, F. García-Alvarez, G. Basáñez, E. Alegre-Aguarón, P. Desportes, L. Larrad, J. Naval, M. J. Martínez-Lorenzo, A. Anel, *Arthritis Rheum.* **2010**, *62*, 2272.

[17] Z. Q. Yuan, K. K. Kolluri, K. H. C. Gowers, S. M. Janes, *J. Extracell. Vesicles* **2017**, *6*, 1.

[18] N. E. Toledano Furman, Y. Lupu-Haber, T. Bronshtein, L. Kaneti, N. Letko, E. Weinstein, L. Baruch, M. Machluf, *Nano Lett.* **2013**, *13*, 3248.

[19] D. De Miguel, A. Gallego-Lleyda, J. M. Ayuso, D. Pejenaute-Ochoa, V. Jarauta, I. Marzo, L. J. Fernández, I. Ochoa, B. Conde, A. Anel, L. Martinez-Lostao, *Cancer Lett.* **2016**, *383*, 250.

[20] D. De Miguel, A. Gallego-Lleyda, A. Anel, L. Martinez-Lostao, *Leuk. Res.* **2015**, *39*, 657.

[21] D. De Miguel, J. Lemke, A. Anel, H. Walczak, L. Martinez-Lostao, *Cell Death Differ. Adv. online Publ.* **2016**, *4*, 1.

[22] O. Seifert, N. Pollak, A. Nusser, F. Steiniger, R. Rüger, K. Pfizenmaier, R. E.

Kontermann, *Bioconjug. Chem.* **2014**, *25*, 879.

[23] A. Nowakowski, K. Drela, J. Rozycka, M. Janowski, B. Lukomska, *Stem Cells Dev.* **2016**, *25*, 1513.

[24] X. Wei, X. Yang, Z. Han, F. Qu, L. Shao, Y. Shi, *Acta Pharmacol. Sin.* **2013**, *34*, 747.

[25] L. Liu, M. A. Eckert, H. Riazifar, D.-K. Kang, D. Agalliu, W. Zhao, *Stem Cells Int.* **2013**, *2013*, 1.

[26] K. Shah, *Adv. Drug Deliv. Rev.* **2012**, *64*, 739.

[27] F. Marofi, G. Vahedi, A. Biglari, A. Esmaeilzadeh, S. S. Athari, *Front. Immunol.* **2017**, *8*, 1770.

[28] O. Levy, W. Zhao, L. J. Mortensen, S. Leblanc, K. Tsang, M. Fu, J. A. Phillips, V. Sagar, P. Anandakumaran, J. Ngai, C. H. Cui, P. Eimon, M. Angel, C. P. Lin, M. F. Yanik, J. M. Karp, *Blood* **2013**, *122*, e23.

[29] J. M. L. Roodhart, L. G. M. Daenen, E. C. A. Stigter, H.-J. Prins, J. Gerrits, J. M. Houthuijzen, M. G. Gerritsen, H. S. Schipper, M. J. G. Backer, M. van Amersfoort, J. S. P. Vermaat, P. Moerer, K. Ishihara, E. Kalkhoven, J. H. Beijnen, P. W. B. Derksen, R. H. Medema, A. C. Martens, A. B. Brenkman, E. E. Voest, *Cancer Cell* **2011**, *20*, 370.

[30] L. Kaneti, T. Bronshtein, N. Malkah Dayan, I. Kovregina, N. Letko Khait, Y. Lupu-Haber, M. Fliman, B. W. Schoen, G. Kaneti, M. Machluf, *Nano Lett.* **2016**, *16*, 1574.

[31] N. Letko Khait, N. Malkah, G. Kaneti, L. Fried, N. Cohen Anavy, T. Bronshtein, M. Machluf, *J. Control. Release* **2019**, *293*, 215.

[32] J. Oieni, L. Levy, N. Letko Khait, L. Yosef, B. Schoen, M. Fliman, H. Shalom-Luxenburg, N. Malkah Dayan, D. D'Atri, N. Cohen Anavy, M. Machluf, *Methods* **2020**, *177*, 126.

[33] X. Li, A. L. Corbett, E. Taatizadeh, N. Tasnim, J. P. Little, C. Garnis, M. Daugaard, E. Guns, M. Hoorfar, I. T. S. Li, *APL Bioeng.* **2019**, *3*, 011503.

[34] T. N. Lamichhane, R. S. Raiker, S. M. Jay, *Mol. Pharm.* **2015**, *12*, 3650.

[35] M. Timaner, N. Letko-Khait, R. Kotsofruk, M. Benguigui, O. Beyar-Katz, C. Rachman-Tzemah, Z. Raviv, T. Bronshtein, M. Machluf, Y. Shaked, *Cancer Res.* **2018**, *78*, 1253.

[36] L. P. Mueller, J. Luetzkendorf, M. Widder, K. Nerger, H. Caysa, T. Mueller, *Cancer Gene Ther.* **2011**, *18*, 229.

[37] M. R. Loebinger, A. Eddaoudi, D. Davies, S. M. Janes, *Cancer Res.* **2009**, *69*, 4134.

[38] M. M. McCarthy, K. A. DiVito, M. Sznol, D. Kovacs, R. Halaban, A. J. Berger, K. T. Flaherty, R. L. Camp, R. Lazova, D. L. Rimm, H. M. Kluger, *Clin. Cancer Res.* **2006**, *12*, 3856 LP.

[39] I. V. Balyasnikova, S. D. Ferguson, Y. Han, F. Liu, M. S. Lesniak, *Cancer Lett.* **2011**, *310*, 148.

[40] Y. Lupu-Haber, T. Bronshtein, H. Shalom-Luxenburg, D. D'Atri, J. Oieni, L. Kaneti, A. Shagan, S. Hamias, L. Amram, G. Kaneti, N. Cohen Anavy, M. Machluf, *Adv. Healthc. Mater.* **2019**, *8*, 1801589.

[41] A. Morizot, D. Mérino, N. Lalaoui, G. Jacquemin, V. Granci, E. Iessi, D. Lanneau, F. Bouyer, E. Solary, B. Chauffert, P. Saas, C. Garrido, O. Micheau, *Cell Death Differ.* **2011**, *18*, 700.

[42] D. Mérino, N. Lalaoui, A. Morizot, P. Schneider, E. Solary, O. Micheau, *Mol. Cell. Biol.* **2006**, *26*, 7046.

[43] A. D. Sanlioglu, E. Dirice, C. Aydin, N. Erin, S. Koksoy, S. Sanlioglu, *BMC Cancer* **2005**, *5*, 1.

[44] L. G. Menon, K. Kelly, H. W. Yang, S.-K. Kim, P. M. Black, R. S. Carroll, *Stem Cells* **2009**, *27*, 2320.

[45] M. de Looff, S. de Jong, F. A. E. Kruyt, *Front. Immunol.* **2019**, *10*, 1.

[46] W. Ouyang, C. Yang, Y. Liu, J. Xiong, J. Zhang, Y. Zhong, G. Zhang, F. Zhou, Y.

Zhou, C. Xie, *Int. J. Oncol.* **2011**, *39*, 1577.

[47] A. Hassanzadeh, M. Farshdousti Hagh, M. R. Alivand, A. A. M. Akbari, K. Shams Asenjan, R. Saraei, S. Solali, *J. Cell. Physiol.* **2018**, *233*, 6470.

[48] J. Lemke, S. von Karstedt, M. Abd El Hay, A. Conti, F. Arce, A. Montinaro, K. Papenfuss, M. A. El-Bahrawy, H. Walczak, *Cell Death Differ.* **2014**, *21*, 491.

[49] D. De Miguel, A. Gallego-Lleyda, P. Galan-Malo, C. Rodriguez-Vigil, I. Marzo, A. Anel, L. Martinez-Lostao, *Clin. Transl. Oncol.* **2015**, *17*, 657.

[50] K. Reimers, C. Radtke, C. Y. Choi, C. Allmeling, S. Kall, P. Kiefer, T. Muehlberger, P. M. Vogt, *Ann. Surg. Innov. Res.* **2009**, *3*, 13.

[51] A. M. K. Law, J. X. M. Yin, L. Castillo, A. I. J. Young, C. Piggin, S. Rogers, C. E. Caldon, A. Burgess, E. K. A. Millar, S. A. O'Toole, D. Gallego-Ortega, C. J. Ormandy, S. R. Oakes, *Sci. Rep.* **2017**, *7*, 15717.

[52] S. Akai, S. Oda, T. Yokoi, *J. Appl. Toxicol.* **2019**, *39*, 451.

[53] B. L. Farah, R. A. Sinha, Y. Wu, B. K. Singh, J. Zhou, B.-H. Bay, P. M. Yen, *PLoS One* **2014**, *9*, e98155.

[54] T. Bronshtein, N. Toledano, D. Danino, S. Pollack, M. Machluf, *J. Control. Release* **2011**, *151*, 139.

[55] W. Y. W. Lee, T. Zhang, C. P. Y. Lau, C. C. Wang, K.-M. Chan, G. Li, *Cytotherapy* **2013**, *15*, 1484.

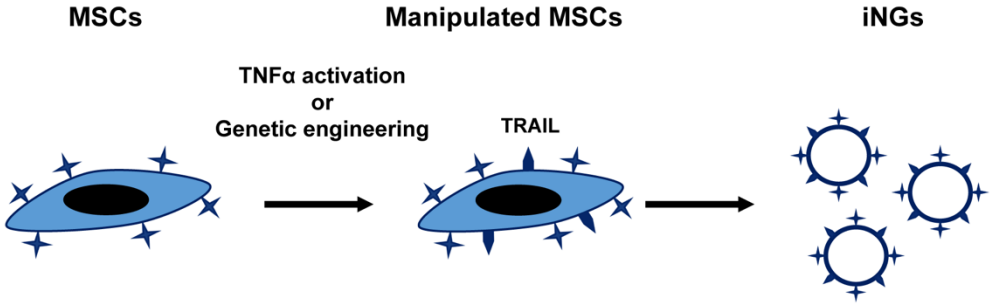

Figure 1. Schematic representation of the manipulation performed on MSCs prior to iNGs production. MSCs were manipulated to express TRAIL by either activation by TNFα or genetic engineering and used as source cells for iNGs production.

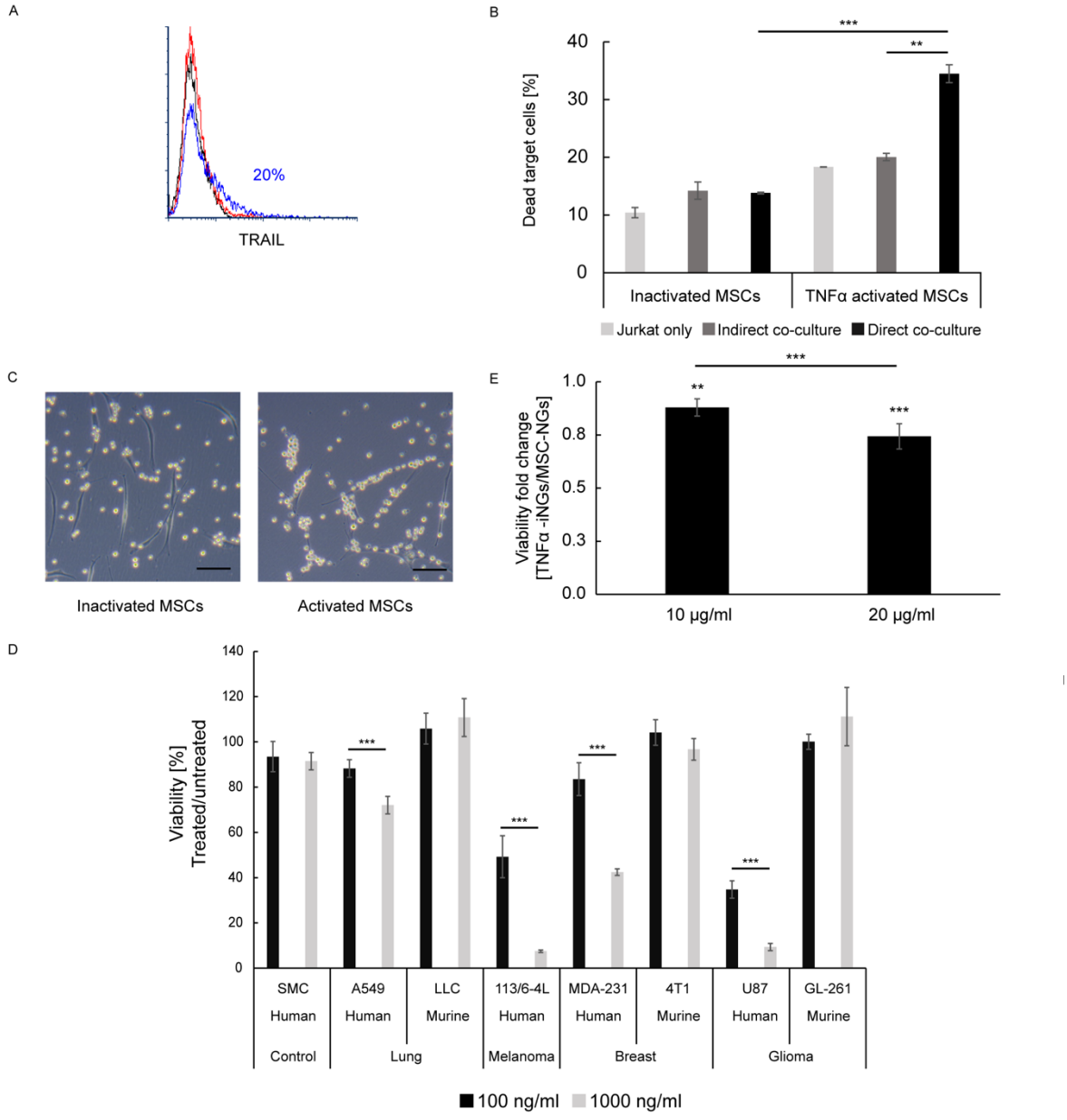

Figure 2. The effect of TNFα-activated MSCs and TNFα-iNGs on cancer cells. A) Representative FACS histogram (n=3) of MSCs activated by TNFα to express TRAIL (blue) and compared to isotype control (red) and unmodified MSCs (black). B) The percentage of dead Jurkat cells after direct (black bar) or indirect (dark gray bar) co-culture with TNFα-activated MSCs for 24 hours. Supernatants were collected, Jurkat cells were incubated with 1 µg/ml PI and were analyzed using flow cytometry. Jurkat cells were used as control (light

gray bar). C) Microscopy images of a 24 hours co-culture of inactivated (left) or TNFα-activated (right) MSCs with Jurkat cells (scale bar 100 µm). D) The viability of cancer cells after 24 hours treatment with 100 ng/ml (black) and 1000 ng/ml (gray) of recombinant human sTRAIL, shown as percentage of viability in respect to untreated control. Cancer cell viability was assessed by AlamarBlue™ assay and measured using a plate reader. SMC were used as a non-cancerous control. E) Fold of change in the viability of MDA-231 cells after 24 hours incubation with TNFα-iNGs and normalized to treatment with MSC-NGs using the same concentration. Viability was assessed by AlamarBlue™ assay and measured using a plate reader. Data are represented as mean ± SD.

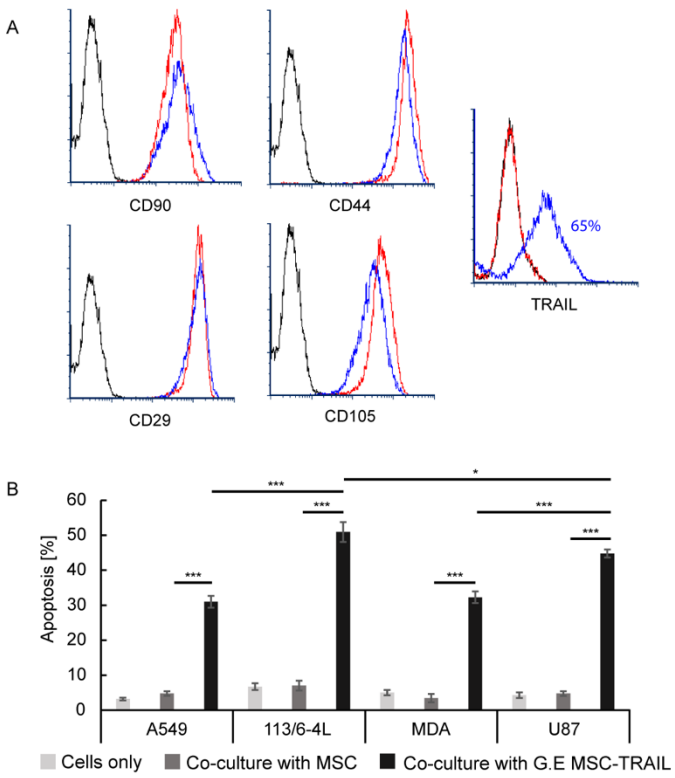

Figure 3. Surface markers and effect of G.E MSC-TRAIL on cancer cells. A) Representative FACS histograms (n=3) of MSC markers and TRAIL expression on G.E MSC-TRAIL (blue). Isotype control (black) and unmodified MSCs (red) were used as controls. B) The percentage of apoptotic cancer cells (Annexin^{+}/PI+) after 24 hours co-culture with G.E MSC-TRAIL (black bar) and compared to co-culture of the cancer cells with natural MSCs (dark gray bar) and cells only (light gray bar) as measured using flow cytometry. Data are represented as mean ± SD.

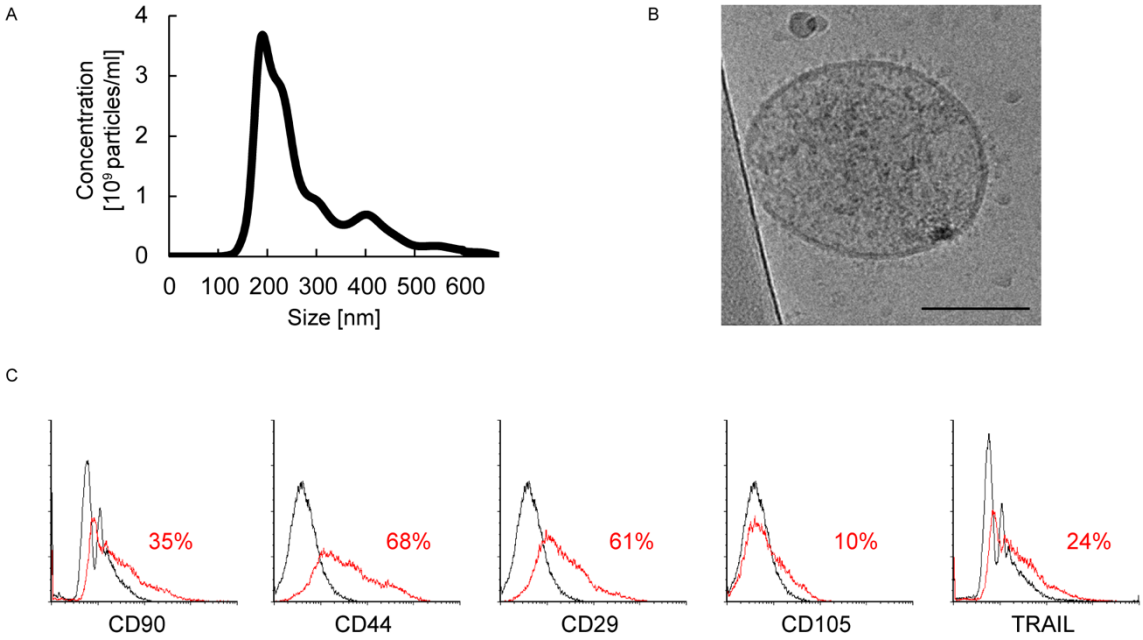

Figure 4. Physical characterization of G.E-iNGs. A) Representative (n>3) size and size distribution of G.E-iNGs as measured by NanoSight. (B) Representative Cryo-TEM image (n>3) of G.E-iNGs (scale bar 100 nm). C) Representative FACS histograms (n=3) of MSC typical markers and TRAIL retention (red curve) on the surface of G.E-iNGs conjugated to Dynabeads, analyzed in flow cytometry, and compared to isotype control (black curve).

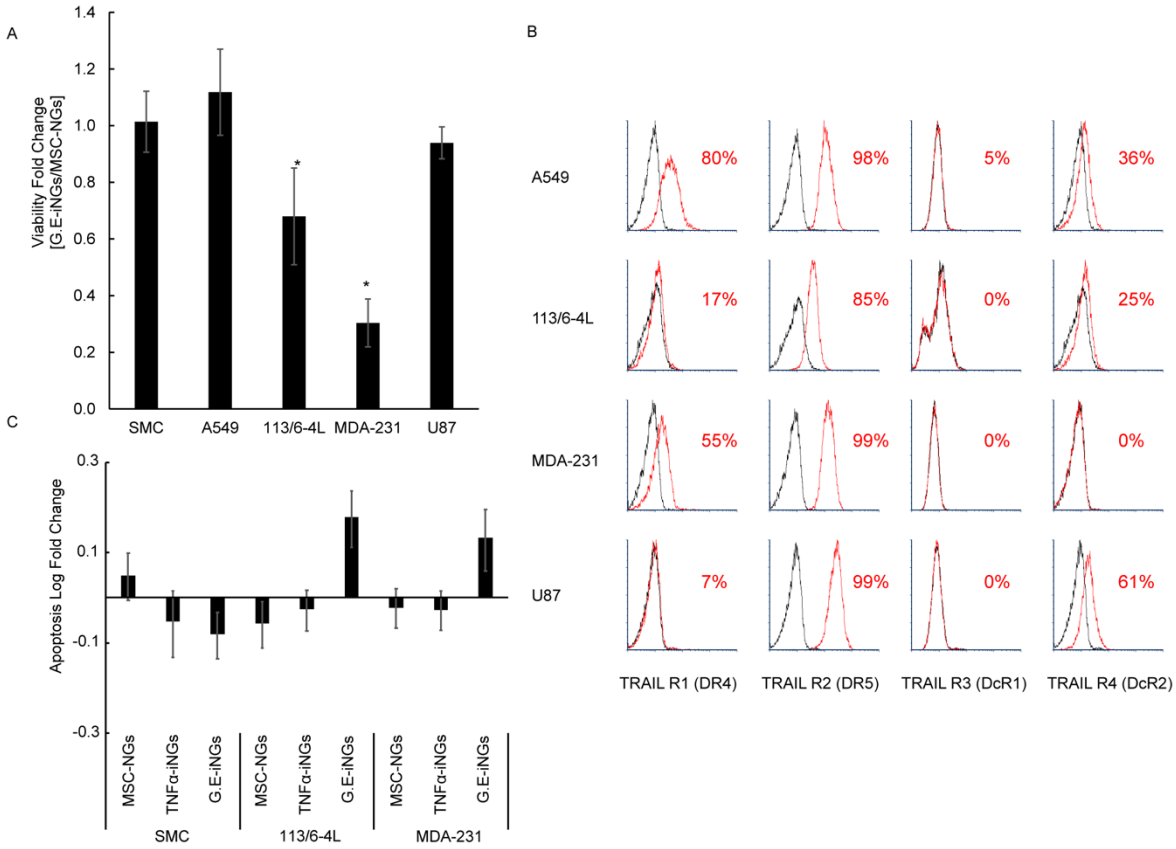

Figure 5. G.E-iNGs effect on cancer cells. A) Fold of change in cancer cells viability after the incubation with G.E-iNGs (10 µg/ml) for 48 hours and normalized to incubation with MSC-NGs. Viability was assessed using AlamarBlue™ and measured using plate reader. B) Representative FACS histograms (n=3) of TRAIL receptors (red curve) on the surface of cancer cells and compared to isotype control (black curve). C) Apoptosis log fold change of 113/6-4L, MDA-231 and SMC control cells after incubation with MSC-NGs, TNFα-iNG and G.E-iNGs (10 µg/ml) for 24 hours as assessed using ApoTox-Glo™ triplex assay. Data are represented as mean ± SD.

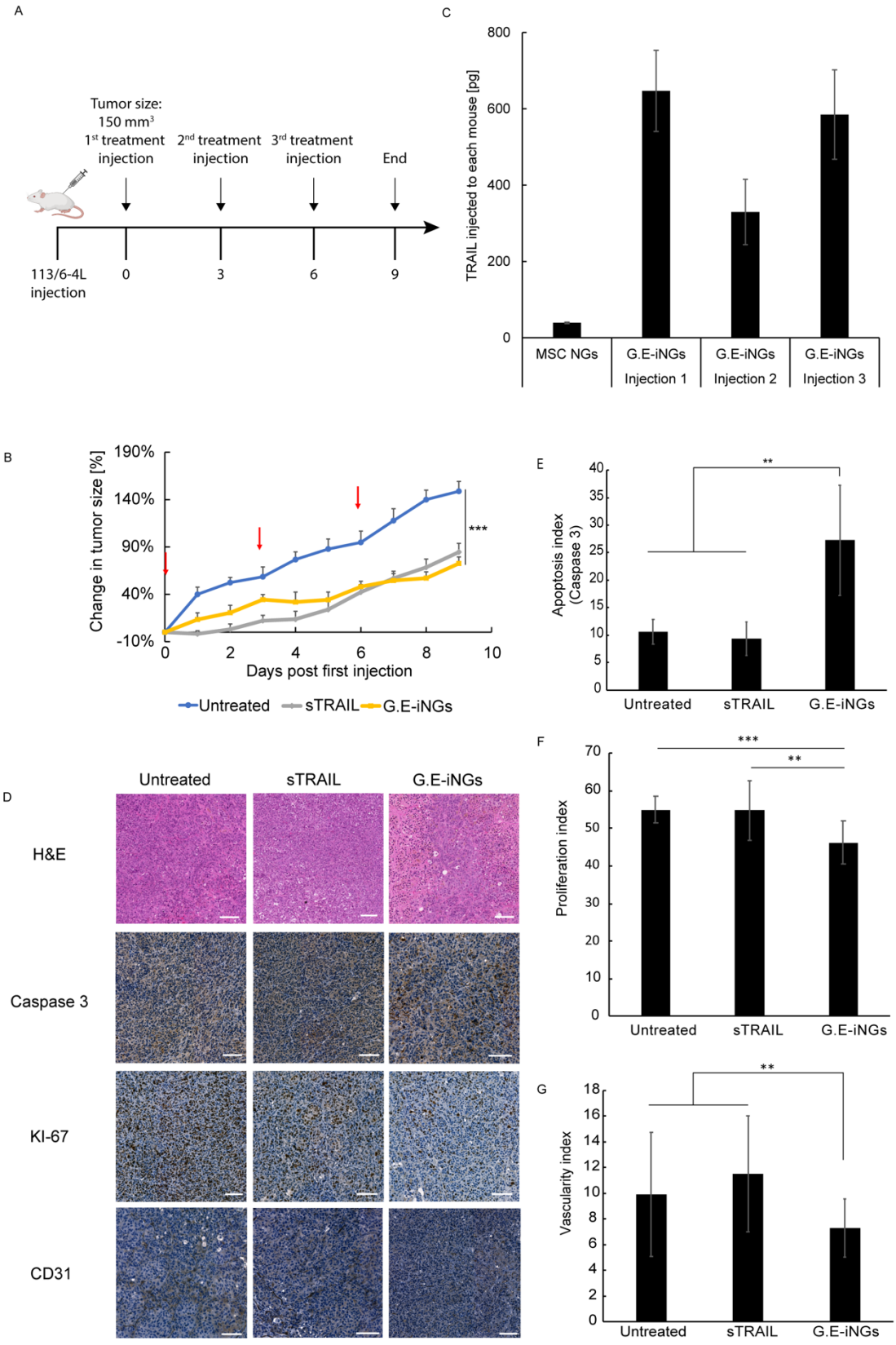

Figure 6. *In-vivo* efficacy studies of G.E-iNGs on human melanoma bearing SCID mice. A) Schematic representation of the efficacy experiment. B) The percentage of change in tumor

size in mice administered with G.E-iNGs or sTRAIL and compared to untreated tumor bearing animals. Data are represented as mean ± SE (n=7 animals per group). C) Amount of TRAIL on the surface of G.E-iNGs, administered to each mouse during the experiment as assessed by ELISA. D) Histopathological (H&E) and immunohistochemical (Caspase 3, Ki67 and CD31) representative micrographs (n=7 mice/group) of tumors harvested from mice administered with G.E-iNGs, sTRAIL and untreated mice (control), 3 days post third administration (scale bar 100 µm). E) Apoptosis (Caspase 3), F) proliferation (Ki67), G) Vascularization (CD31) indices calculated by image analysis using Andy's algorithm of IHC micrographs of tumors harvested from mice administered with G.E-iNGs, sTRAIL and untreated mice (control), 3 days post third administration (n=30 samples/group). Data are represented as mean ± SD.

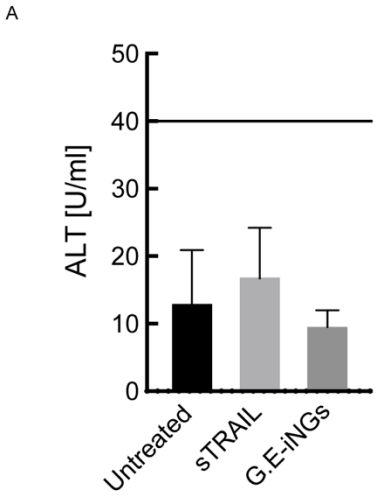

B

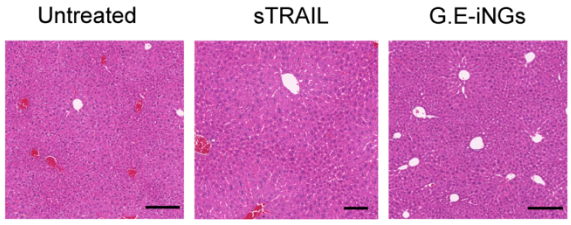

C

Cytokin (pg/ml)	Untreated	Week 1 p.a	Week 3 p.a
IFN-γ	<2.56	<2.56	<2.56
IL-1b	0.44±0.53	<0.42	<0.42
IL-6	4.80±5.15	2.80±1.29	5.7±5.35
TNF-α	<0.32	<0.32	<0.32

Figure 7. *In-vivo* safety studies of G.E-iNGs. A) ALT levels (U/ml) in the serum of SCID mice bearing human melanoma model after iNGs or control treatments. ALT levels were assessed using Alanine Transaminase Colorimetric Activity Assay Kit and measured in plate reader. Black line represents toxic ALT level. B) Representative histological (H&E) micrographs of livers harvested from untreated or treated tumor bearing SCID mice with iNGs or sTRAIL control (scale bar 100 µm). C) Cytokines levels of untreated or treated C57BL mice 1- or 3-weeks post administration (p.a) of G.E-iNGs. Cytokines levels were assessed using Milliplex Mouse Cytokine/Chemokine Magnetic Bead Panel. Data are represented as mean ± SD.

Author biography

Lior Levy received his Ph.D in Biotechnology and Food Engineering from the Technion—Israel Institute of Technology in 2020, under the supervision of Prof. Marcelle Machluf, focusing on the development of Immunotherapeutic NGs to treat cancer. He is currently a post-doctoral fellow at the National Cancer Institute (NCI) at the NIH.

Marcelle Machluf is dean of the Faculty of Biotechnology and Food Engineering at Technion Haifa Israel, the head of the laboratory for Cancer Drug Delivery and Cell Based Technologies, and the president of the Israel Chapter of the Controlled Release Society. She holds a Ph.D. degree in biotechnology from the Faculty of Chemical Engineering at Ben-Gurion University Beer-Sheva and was a post-doctoral fellow at Harvard Medical School under the supervision of Prof. Anthony Atalla. She joined the Technion in 2001, and since then, her laboratory has developed and engineered biomedical platforms for drug delivery and regenerative medicine.